

# Dynamic self-assembly of coordination polymers in aqueous solution

Cite this: *Soft Matter*, 2014, 10, 5231

Wen Li,\* Yongju Kim, Jingfang Li and Myongsoo Lee\*

The construction of supramolecular polymers has been intensively pursued because the nanostructures formed through weak non-covalent interactions can be triggered by external stimuli leading to smart materials and sensors. Self-assemblies of coordination polymers consisting of metal ions and organic ligands in aqueous solution also provide particular contributions in this area. The main motivation for developing those coordination polymers originates from the value-added combination between metal ions and ligands. This review highlights the recent progress of the dynamic self-assembly of coordination polymers that result from the sophisticated molecular design, towards fabricating stimuli-responsive systems and bio-related materials. Dynamic structural changes and switchable physical properties triggered by various stimuli are summarized. Finally, the outlook for aqueous nanostructures originated from the dynamic self-assembly of coordination polymers is also presented.

Received 16th May 2014

Accepted 3rd June 2014

DOI: 10.1039/c4sm01068j

[www.rsc.org/softmatter](http://www.rsc.org/softmatter)

## 1 Introduction

Supramolecular polymers produced *via* non-covalent interactions represent important progress in the fields of chemistry and materials science.<sup>1–4</sup> They possess not only traditional polymer properties but also distinctly new features. For example, their molar mass distribution is broadly varied, and strongly dependent on the concentration.<sup>5,6</sup> The most important feature is the relatively low activation energy of the non-covalent interactions, that implements dynamic motion into supramolecular polymers and endows this system with stimuli-responsiveness and adaption.<sup>7–9</sup> The rational design and synthesis of supramolecular polymers are undoubtedly important and the primary concern with current research is towards engineering the polymers with unprecedented properties. There are different non-covalent interactions available for the synthesis of supramolecular polymers.<sup>2,4,10,11</sup> Among them, metal–ligand coordination is particularly attractive as the coordinative bond is highly specific and directional.<sup>12,13</sup> Coordination polymers, employing a metal-ion coordination interaction to hold the monomers together, have attracted immense research interest because the broad catalogue of metal ions comprising nearly half the periodic table offers a very flexible choice in the molecular design. More interestingly, the properties of metal ions such as charge, color, luminescence, magnetism, redox behavior, and catalysis can be incorporated into polymer networks with the aim of developing multi-functional materials.<sup>14–16</sup> Additionally, the binding strength of the metal–ligand

interaction can be readily tuned with the appropriate combination of ligands and metal ions.<sup>17</sup> In general, the binding strength of polydentate ligands is higher than that of monodentate ligands. Furthermore, the thermodynamic and kinetic stabilities of metal complexes rely on the nature of metal ions. Most complexes formed from second and third row transition metal ions, such as platinum, palladium or ruthenium, are kinetically stable in solution.<sup>18</sup> However, those complexes consisting of first row transition metals ions are kinetically labile, which means they have a strong propensity to dissociate and associate under the influence of chemical and physical triggers, such as, solvents,<sup>19</sup> temperature,<sup>20</sup> ultra-sonication,<sup>21</sup> pH,<sup>22</sup> redox reactions,<sup>23</sup> and competitive ligands.<sup>24</sup> Continuing this theme, the construction of dynamic self-assembled nanostructures in solution from the synthetic coordination polymers have been rapidly emerging as types of smart supramolecular materials with tailored properties.<sup>25–28</sup>

Although several articles have presented a systemic summary of the dynamic motion of the coordination polymers, most of them focus on the self-assembled nanostructures in organic media.<sup>17,29–36</sup> This limits their further applications, especially in biological systems, which require self-assembly to occur in water. It has long been known that water, serving as a kind of environmentally friendly solvent, is ubiquitous and indispensable for the existence of a biological system. The dynamic supramolecular self-assembly of biomolecules in aqueous solution has significant potential in controlling many biological events, such as intracellular transport and cell division.<sup>37,38</sup> Some proteins, especially those containing prominent metal ion binding sites, perform their bio-functions through the dynamic self-assembly triggered by metal ions.<sup>39</sup> In this system, metal ions play a crucial role in the stabilization of the protein

State key laboratory of supramolecular structure and materials, Jilin University, Changchun, 130012, China. E-mail: wenli@jlu.edu.cn; mslee@jlu.edu.cn; Fax: +86 431-85193421; Tel: +86 431-85168499

structure,<sup>40</sup> induction of conformational transitions from the unfolded to the folded state or between different folded states,<sup>41</sup> improvement of molecule transport and enzymatic catalysis,<sup>42,43</sup> and adjusting the disease-related process.<sup>44</sup> Inspired by the complex and intriguing bio-systems, a lot of research has been made to develop aqueous self-assembly based on the coordination polymers with different molecular architectures, including main-chain, side-chain, star-like and branched polymers.<sup>45–50</sup> Emphasis has been placed on two aspects: one is that the dynamic self-assembly nanostructures respond to different stimuli, and the other is the switchable physical properties. Normally, this change is fully reversible once the external stimulus has been removed.

In this paper, we focus on the recent progress in the development of aqueous self-assembly from the coordination polymers. We will touch upon the different types of water-soluble coordination polymers with dynamic nanostructures, physical properties and functionality. We start this presentation from the dynamic polymerization and depolymerization behavior of coordination polymers in water. We show how these self-assembled nanostructures exhibit switchable motion. Then, we move on to smart functional materials based on the switchable self-assembly. We highlight some possible applications in the fields of molecular sensors and bioassays.

## 2 Dynamic polymerization and depolymerization of coordination complexes in aqueous solution

Pyridine is known to display a high binding affinity to many metal ions.<sup>17</sup> To fabricate a coordination polymer in aqueous solution, the pyridine-based ligands should be structurally modified with water-soluble groups. With this idea in mind, a bifunctional ligand (**L1**, Fig. 1a), consisting of two terpyridine groups bridged by a poly(ethylene oxide) (PEO) spacer was synthesized by van der Gucht *et al.*<sup>51</sup> Preparation of the main-

chain coordination polymer was performed in a straightforwardly through the addition of  $\text{Cd}(\text{NO}_3)_2$  into a aqueous solution of **L1** under ambient conditions. In contrast to the preparation procedures, the characterization of the coordination polymers was not easy because of the dynamic polymerization. The complex formation between the terpyridine ligand groups and  $\text{Cd}^{2+}$  ions was demonstrated using ultraviolet/visible (UV/vis) spectroscopy and potentiometric titration. Viscometry and voltammetry were used to study the formation of cadmium-based coordination polymers. The authors suggested that the bifunctional ligands can form not only linear polymers through metal ion coordination, but also cyclic oligomers (Fig. 1a). In another example, Vermonden *et al.* synthesized a water-soluble bolaform ligand (**L2-*n***,  $n = 4, 6$ ), where pyridine-2,6-dicarboxylic acid groups are connected at the 4-position of the pyridine ring by tetra- and hexa-ethylene oxide spacers (Fig. 1b).<sup>45</sup>  $^1\text{H-NMR}$  and viscosity measurements suggested that the bifunctional ligands also formed linear polymers as well as cyclic conformations when  $\text{Zn}(\text{ClO}_4)_2$  was added into the aqueous solution of **L2-*n*** (Fig. 1). The amount of linear polymers depends on the concentration, temperature, and the molar ratio between the metal ion and the ligand molecules. At low concentrations, most ligands are incorporated in to cyclic conformations, while linear polymer chains are more dominant at higher concentrations. With increasing temperature, the amount of the polymer chains becomes larger, which causes an unusual increase in viscosity. However, when lanthanide ions such as  $\text{La}^{3+}$  and  $\text{Nd}^{3+}$  were used to combine with the same ligand (**L2-*n***), three-dimensional (3-D) polymer networks were obtained at high concentrations (Fig. 1b).<sup>52</sup> This is because the lanthanide ions are larger in size and can accommodate 9-coordination, which can bind three terdentate ligand groups by self-assembly, giving rising to the formation of a 3-D network with high viscosity. With decreasing concentration, the 3-D polymer network transforms into a linear structure, as shown in Fig. 1b. Interestingly, the addition of  $\text{Zn}^{2+}$  to the linear polymers  $\text{Nd}^{3+}/\text{L2-*n*$  led to decreased viscosity,<sup>53</sup> suggesting that divalent metal ions added to a system consisting of terdentate bifunctional ligands and lanthanide ions might act as “chain stoppers”. It is clear that  $\text{Nd}^{3+}$  binds three ligand groups, while  $\text{Zn}^{2+}$  binds only two ligand groups. Thus, the addition of  $\text{Zn}^{2+}$  into the  $\text{Nd}^{3+}/\text{L2-*n*$  polymer system will lead to the formation of a cyclic end cap as depicted in Fig. 1b, which reduces the average chain length and the solution viscosity as well. The above results demonstrate that the polymerization of coordination complexes is dynamic and strongly dependent on the concentration, temperature and the nature of metal ions. The dynamic behaviour of the polymers is attributed to the kinetically labile coordination interaction.

To obtain a kinetically stable coordination polymer, one should consider the second or third row transition metal ions as crosslinking junctions because their association constants are high enough to hold the polymer backbone together in polar solution. Schubert *et al.* reported an AB diblock copolymer (Fig. 2) based on a kinetically stable terpyridine–ruthenium(II) interaction.<sup>54,55</sup> A mono-chelic terpyridine ligand with a PEO tail (**L3**) was firstly complexed with  $\text{RuCl}_3$ . The resultant mono-

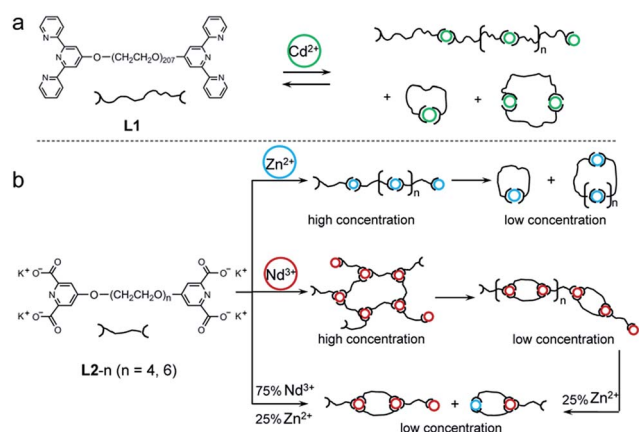


Fig. 1 (a) Schematic molecular structure of ligand **L1** and the corresponding coordination polymer with  $\text{Cd}^{2+}$  ions and (b) molecular structure of **L2** and the dynamic polymerization with metal ions. Reproduced with permission from ref. 45, 51, 52 and 53. Copyright 2003 and 2004 American Chemical Society, 2004 Wiley-VCH.

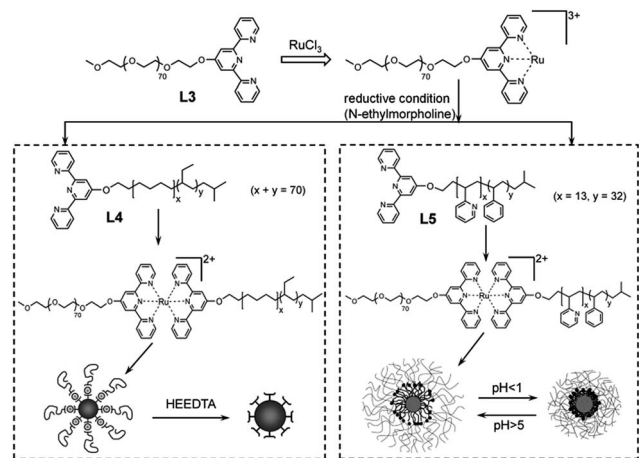


Fig. 2 Schematic molecular structures of ligands **L3**, **L4** and **L5**, and the resultant coordination polymers formed upon addition of  $\text{Ru}^{2+}$  ions. Reproduced with permission from ref. 55 and 56. Copyright 2002 American Chemical Society, 2002 Wiley-VCH.

complex was then reacted with the terpyridine-terminated poly(ethylene-*co*-butylene) (PEB) block copolymer (**L4**) under reductive conditions, giving rise to the target coordination copolymer. The copolymer obtained can self-assemble into a stable micelle in water with a PEB core and PEO shell. However, the addition of a competitive ligand, hydroxyethylethylenediaminetriacetic acid sodium salt (HEEDTA) can chelate with the  $\text{Ru}^{2+}$  ions and lead to the dissociation of the diblock copolymer. In an extension of this work, the authors introduced functional groups into the organic ligand to establish a pH-sensitive feature.<sup>56</sup> In this case, a diblock ligand terpyridine-terminated poly(styrene)-*b*-2-vinylpyridine ( $\text{PS}_{32}$ - $\text{P2VP}_{13}$ ) (**L5**) was combined with **L3** through an  $\text{Ru}^{2+}$  ion junction, resulting in the formation of an ABC triblock copolymer (Fig. 2). Core-shell-corona micelle assemblies with an approximate diameter of 80 nm were observed when the ABC copolymer was dissolved in acidic water ( $\text{pH} = 1$ ). However, a very significant decrease in micelle size was observed when the pH value of the aqueous solution was increased to  $\text{pH} = 5$ , in agreement with the acid dissociation constant ( $\text{pK}_a$ ) of P2VP units. The relatively large size of the coordination copolymer micelles in acidic solution originates from the electrostatic repulsion between the protonated P2VP segments. When the pH value increases to 5, the electrostatic repulsion effect was strongly suppressed accompanied with the neutralization of P2VP segments, giving rise to contracted micelles. The switchable expansion and contraction of the micelles can be triggered by pH or ionic strength. Following a similar strategy, thermo-sensitive coordination copolymers can also be synthesized by modifying the terpyridine ligand with a poly(*N*-isopropylacrylamide) chain.<sup>57</sup>

The above examples demonstrate that the organic ligands modified with functional groups endow the resultant coordination polymers with additional features. It is therefore expected that complementary binding interactions could be combined with the coordination bond to obtain multi-responsive supramolecular polymers in water. Gröger *et al.* designed a

heteroditopic ligand (**L6**) in which a terpyridine ligand was attached to a guanidiniocarbonyl pyrrole carboxylate zwitterion.<sup>58</sup> When  $\text{Fe}^{2+}$  ions were added into an aqueous solution of **L6** within a pH range from 5 to 7, large linear polymers with a considerable length of 100 nm were observed. The dependence of viscosity *versus* the concentration showed the presence of a critical polymerization concentration (CPC) in this system. Below the CPC, the coordination complex formed mainly cyclic oligomers accompanied with some linear structures in the equilibrium state. Above the CPC, linear polymer chains became more favourable at the expense of the cyclic ones. The dynamic properties of the resulting supramolecular polymers were further evaluated with a variety of external stimuli. As shown in Fig. 3, ligand **L6** can reversibly change from monomer to a metal complex dimer or ion paired dimer and finally to supramolecular polymer depending on the simultaneous absence or presence of both chemical stimuli (pH and  $\text{Fe}^{2+}$ ).

Protein can be considered as a new kind of ligand for performing the coordination polymerization process because of easy structural modification. Chaperonin GroEL, a barrel-shaped tetradecameric protein assembly, was site specifically modified in the entrance parts of its cavity with a number of spiropyran (SP) units (Fig. 4).<sup>59</sup> When the modified protein  $\text{GroEL}_{\text{SP}}$  was dissolved in an acidic buffer solution, the colourless solution gradually turned light-purple because of the partial isomerization of SP to merocyanine (MC). Interestingly, the addition of divalent metal ions, such as  $\text{Ca}^{2+}$ ,  $\text{Co}^{2+}$ ,  $\text{Mg}^{2+}$ ,  $\text{Zn}^{2+}$ , into the mixed aqueous solution of  $\text{GroEL}_{\text{SP}}$  and  $\text{GroEL}_{\text{MC}}$  caused one-dimensional (1-D) polymerization of the protein  $\text{GroEL}_{\text{MC}}$ . As shown in Fig. 4, micrometer long nanotubes with a uniform diameter of 15 nm were observed from a transmission electron microscopy (TEM) image. However, it was difficult to induce the 1-D polymerization using monovalent cations, such as  $\text{Cs}^+$ ,  $\text{K}^+$  and  $\text{Na}^+$ . The comparison experiment demonstrates that divalent metal ions can coordinate with the MC groups to drive the supramolecular polymerization of  $\text{GroEL}_{\text{MC}}$ . The polymerized nanotubes are thermodynamically stable since they are formed by multiple coordination interactions. The metal ions can be removed by the addition of a stronger

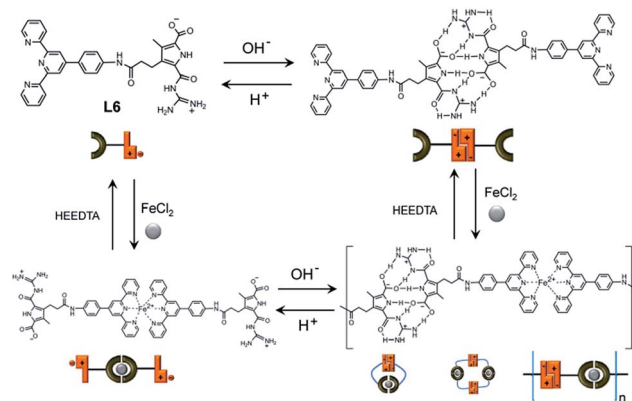


Fig. 3 Schematic molecular structure of ligand **L6**, and the dynamic polymerization of the metal–ligand complex. Reproduced with permission from ref. 58. Copyright 2011 American Chemical Society.

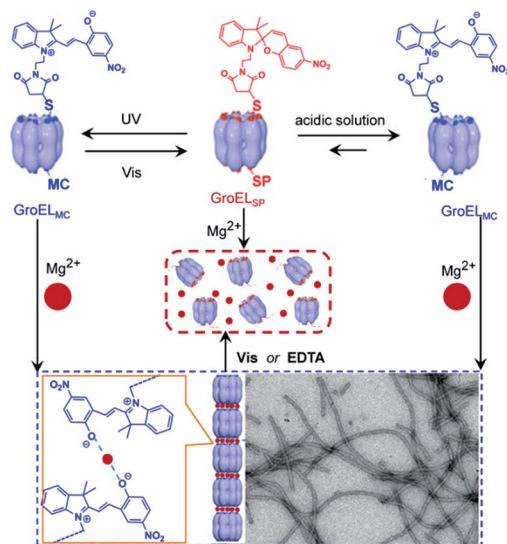


Fig. 4 Schematic illustrations of protein GroEL<sub>SP</sub> carrying multiple spiropyran (SP) units at its apical domains and the isomerized protein GroEL<sub>MC</sub>. TEM image of the coordination polymers with nanotubular structures upon addition of divalent metal ions, and their depolymerization triggered by visible light or competitive ligands. Reproduced with permission from ref. 59 and 60. Copyright 2009 and 2013 American Chemical Society.

chelator, such as ethylenediaminetetraacetic acid (EDTA), causing the dissociation of the 1-D polymer into monomeric units. Additionally, the isomerization of SP and MC under irradiation with alternate UV and visible light is another strategy to mediate the polymerization and depolymerization of 1-D nanotubes.<sup>60</sup> When acidic buffer solution of GroEL<sub>SP</sub> containing a mixture of MgCl<sub>2</sub> and dithiothreitol (DTT) was continuously exposed to UV light for 15 min, a 1-D polymer with a nanotube structure was observed because of the coordination interactions between Mg<sup>2+</sup> and the isomerized GroEL<sub>MC</sub>. However, the long nanotubes disappeared completely after the polymer solution was exposed to visible light ( $\lambda > 400$  nm) for 15 min. Only some oligomeric fractions containing monomer up to hexamer were observed. Meanwhile, subsequent exposure of the scission mixture to UV light resulted in the recovery of the tubular polymers (Fig. 4 left hand side). It is worth noting that the presence of DTT in this protein solution is necessary to ensure such a light-mediated reversible polymerization occurs because the DTT can remove the radicals generated from the MC analogue upon photoexcitation.

### 3 Switchable nanostructures based on self-assembled coordination polymers

Apart from the dynamic association and dissociation response to external stimuli, the coordination complexes have the ability to self-assemble into ordered hierarchical nanostructures with a switchable motion. In particular, helical architectures formed from the self-assembly of coordination polymers have attracted

increasing interest.<sup>61–64</sup> The skewed conformation of 3,3'-oxybispyridine (L7) with a non-rigid interannular dihedral angle is favourable for the formation of a linear polymer by coordination to the silver(I) ion.<sup>65</sup> Crystallographic characterization revealed that the polymer framework adopted a helical conformation with its counter anions pinched in two columns inside the helix, as described in Fig. 5. Interestingly, the helical pitch of the coordination polymer could be tuned through the reversible incorporation of guest counter anions in aqueous solution. The switchable contraction and expansion of the helical pitch is exactly proportional to the volume of the guest anions.

In another example, the contraction-expansion helix was fabricated from the dynamic self-assembly of a synthetic coordination polymer triggered by pH and competitive ligands.<sup>66</sup> As shown in Fig. 6, a coordination polymer, consisting of semi-artificial curdlan ( $\alpha$ -1,3-glucan) featuring a dendritic amphiphilic Zn-chlorophyll unit attached laterally to the main chain of repeated glucose units, self-assembled into a helical conformation in aqueous solution because the stacking among the peripheral chlorophyll units along the main chain together with the directional Zn–O coordination interactions promoted the formation of a helix. Upon addition of a competitive pyridine ligand, the stacking of chlorophyll units dissociated into monomeric states in water because of the strong coordination force through Zn–N, leading to an expansion of the helical pitch. A systemic investigation showed that the helical pitch could be elongated further through lengthening the added ligands, such as the 1,2-di-(4-pyridyl)ethylene and 4,4'-(*p*-phenylenebisvinylene)bispyridine. The degree of extension of the helical polymer is also proportional to the length of the added ligands. Significantly, the extended helical conformation of the coordination polymer can directly return to its contracted form by decreasing the pH value because the protonation of pyridine-based ligands led to their removal from the chiral groove constructed by the chlorophyll units.

Lee *et al.* reported a kind of helical coordination polymer in aqueous solution which displayed switchable extension-

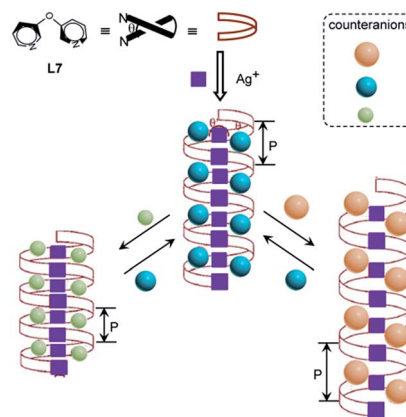


Fig. 5 Molecular structure of L7 and the schematic representation of the switchable helix of the resultant coordination polymer triggered with the competitive counter anions. Reproduced with permission from ref. 65. Copyright 2000 American Chemical Society.

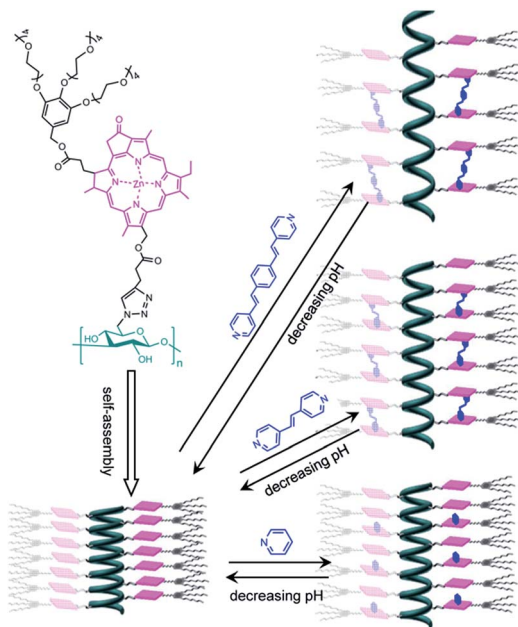


Fig. 6 Molecular structure of the coordination polymer, and the contraction-expansion helix triggered by the competitive ligands and pH. Reproduced with permission from ref. 66. Copyright 2013 Wiley-VCH.

contraction motion which was triggered by temperature.<sup>67</sup> Bent pyridine ligands (**L8**, **L9**) with oligoether dendrons were complexed with silver trifluoromethanesulfonate ( $\text{AgOTf}$ ) in aqueous solution to give the coordination polymers (Fig. 7). The quenched fluorescence spectra indicated that the aromatic segments formed strong aggregates. The circular dichroism (CD) spectra of the coordination polymer solution revealed the formation of a helical structure with a preferred handedness. The TEM image of the metal complexes with a negative stained sample showed elementary cylindrical fibers with lengths of several micrometers. The shape of the 1-D nanostructure remained unchanged upon heating. However, there was a significant decrease in the cross-sectional dimensions of the cylindrical objects at high temperature. The UV and CD spectra showed that the coordination polymers adopted an elongated conjugation length upon heating. The NMR experiments

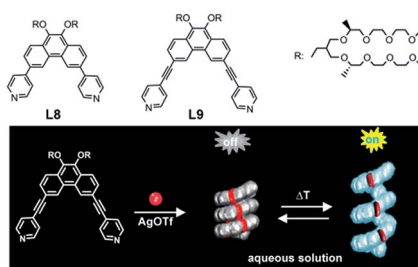


Fig. 7 Molecular structures of ligand **L8** and **L9**, and the schematic illustrations of the helical coordination polymer with dynamic motion triggered by temperature. Reproduced with permission from ref. 67. Copyright 2007 American Chemical Society.

demonstrated that the helical polymer strands were elongated because of the lower critical solution temperature (LCST) behaviour of the ethylene oxide chains in aqueous medium. At temperatures above the LCST, the ethylene oxide chains would be dehydrated and then collapse into a molecular globule because of the loss of the hydrogen bonding between ether oxygens and water molecules. The steric crowding of the globules drove the helical strands to be extended. Significantly, an enhanced emission was observed in the polymer solution upon heating, which was indicative of the separation between the adjacent aromatic units within the helical fiber because of the breakup of the  $\pi$ - $\pi$  stacking interactions. At temperatures below the LCST, the extended helix returned to its original contracted state. Correspondingly, the strong emission of the polymer solution was quenched again upon cooling. Such extension and contraction motion of the coordination polymers may offer intriguing possibilities for the development of artificial machines and optical sensors.

Jiang *et al.* also reported a new kind of coordination polymer sensor created using an elaborate molecular design.<sup>68</sup> A linear coordination polymer was firstly synthesized by mixing cysteine (**Cys**; **L10**) and  $\text{AgNO}_3$  in aqueous solution. As shown in Fig. 8, a zigzag main-chain backbone was stabilized by the strong Ag-S coordination interaction. At pH = 5, the aqueous solution of the polymer showed a luminescent emission at 545 nm because of the ligand-to-metal charge-transfer transition mixed with the metal-centered (ds/dp) state that was modified by the argentophilic interaction (ligand-to-metal-metal charge transfer). This is an indication of the synergetic interplay of the electrostatic interaction among the Cys side units and the Ag(I)-Ag(I) argentophilic attraction in the polymeric backbone. More importantly, the emission of Ag(I)-Cys solution at 545 nm gradually decreased and eventually disappeared with increasing pH. This phenomenon can be explained by the electrostatic interactions among Cys residues in the polymeric backbone. The electrostatic attraction of the Cys residues at low pH would give a smaller Ag-S-Ag angle ( $\alpha_1$ ) than that ( $\alpha_2$ ) at high pH when the electrostatic repulsion occurs. The Ag(I)-Ag(I) argentophilic attraction was accordingly weakened because of the enlarged distance in a high pH solution. These processes could be reversed by lowering the solution pH, and such switching motion could be repeated for several cycles without an obvious

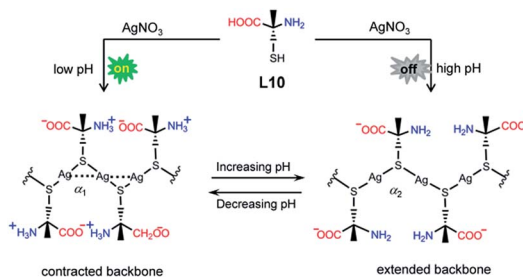


Fig. 8 Schematic representation of the ligand **L10** and the resultant coordination polymer with switchable luminescence. Reproduced with permission from ref. 68. Copyright 2011 American Chemical Society.

loss of luminescent signal. This strategy could be extended to Cu(I)-Cys and Au(I)-Cys systems, indicating that the M(I)-SR coordination polymers ( $M = \text{Ag}, \text{Au}, \text{or Cu}$ ) are able to serve as spectral sensing platforms.

In addition to the dynamic contraction–expansion motion, reversible structural transition is also useful if the aim is to create smart nanomaterials. Lee *et al.* developed a type of coordination polymer with a structural transition feature triggered by competitive anions.<sup>69</sup> A bent-shaped rod segment containing pyridine units at both ends was modified by grafting hydrophilic oligoether dendrons at the apex position (Fig. 9). The resultant water-soluble ligands (**L11** and **L12**) were complexed with silver tetrafluoroborate ( $\text{AgBF}_4$ ) to give right-handed helical polymers with elongated fiber structures in aqueous solution. The polymer solution underwent spontaneous gelation at concentrations above 2.5 wt%, suggesting that the helical fibers formed an entangled fibrillar network which immobilized the water molecules. However, upon addition of 1 equivalent of  $\text{Bu}_4\text{N}^+\text{C}_2\text{F}_5\text{CO}_2^-$ , the elongated fibers transformed into discrete ribbon-like aggregates accompanied with a rapid collapse of the polymer gel (Fig. 9). The CD spectra indicated that the helical conformation of the polymers changed into an unfolded zigzag conformation on replacing  $\text{BF}_4^-$  with  $\text{C}_2\text{F}_5\text{CO}_2^-$  ions. It is clear that the size of the counter anion has a profound effect on the self-assembled nanostructures and the macroscopic properties of the polymers. In an alternative way, removal of the  $\text{Ag}^+$  by adding tetra-*n*-butylammonium fluoride to the polymer also caused a rapid collapse of the gel through the depolymerization of the polymer chain.

To explore further the dynamic features, the researchers synthesized an amphiphilic ligand (**L13**) consisting of a longer bent-shaped rod segment containing *m*-pyridine units at both ends and a hydrophilic oligoether dendron with an S configuration grafted at the apex (Fig. 10).<sup>70</sup> The TEM image of **L13** showed flat sheets with regular stripes having a periodicity of 2 nm, suggesting that the aromatic units of **L13** adopted a zigzag

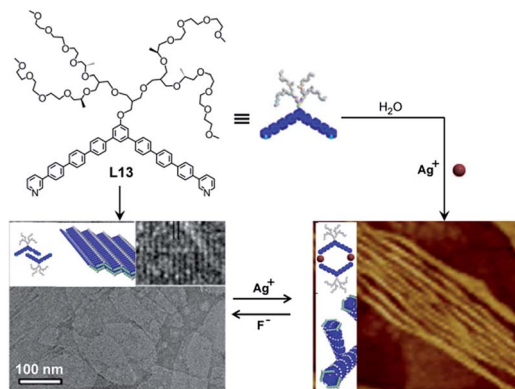


Fig. 10 Molecular structure of **L13**, TEM, AFM images and the schematic structure transition of the corresponding coordination polymer. Reproduced with permission from ref. 70. Copyright 2013 American Chemical Society.

conformation with a parallel orientation to the sheet plane (Fig. 10). The CD spectra of the aqueous solution of **L13** displayed a silent Cotton effect even with the presence of chiral side groups, which was predictable for symmetrical two-dimensional (2-D) objects. However, the addition of silver salt to the solution of **L13** induced significant CD signals. TEM and atomic force microscopy (AFM) analysis confirmed that the 2-D sheets transformed into a 1-D helical tubule. Interestingly, the concentration-dependent TEM measurements showed that the coordination interaction between the Ag(I) ion and the pyridine groups led to the formation of achiral macrocycles in diluted aqueous solution. With increasing concentration, the dimeric macrocycles stacked on top of each other to form chiral tubules (Fig. 10). Another interesting point is that the structural transformation between 1-D helical tubules and 2-D flat sheets could be mediated reversibly through alternated addition of  $\text{F}^-$  and  $\text{Ag}^+$ .

## 4 A smart hydrogel based on the dynamic self-assembly of a coordination polymer

Supramolecular hydrogels with stimuli-responsive properties have significant potential in the development of smart devices and biomaterials.<sup>71,72</sup> Hydrogels obtained from the self-assembly of coordination polymers provide new opportunities to introduce the properties of metals, such as luminescence, magnetism, and catalytic and redox behaviour, into soft materials.<sup>17,73–75</sup> Pioneering work in the field of coordination hydrogels was performed by Chujo *et al.*<sup>76</sup> The coordination complex formation and the gelation occurred after addition of Co(II) salt to the aqueous solution of bipyridyl-modified polyoxazoline (**L14**). The gels obtained, dissolved rapidly at higher temperatures. However, at the same temperature, the Co(III) complex gels were stable. The difference in stability of the coordination gels allows the development of a smart hydrogel triggered by the redox reaction of cobalt ions. It is clear that the kinetic stability

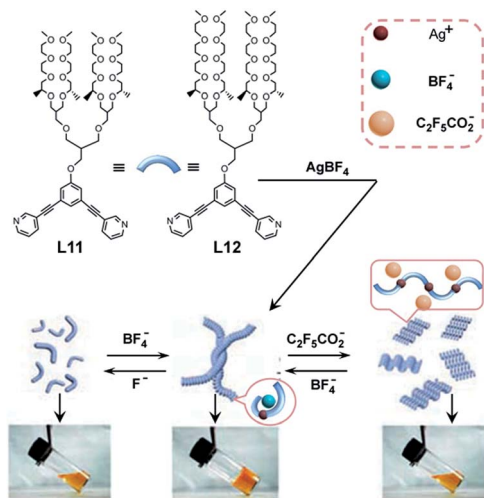


Fig. 9 Molecular structures of **L11** and **L12**, and the schematic illustrations of the structural transition of the coordination polymer. Reproduced with permission from ref. 69. Copyright 2005 Wiley-VCH.

of the cobalt complexes depends on the oxidation state of the metal ions. In the case of divalent cobalt ions, the metal–ligand interactions were kinetically labile, which caused the ligand exchange reaction in the polymers from the intermolecular crosslinks to the intramolecular ones (Fig. 11). Furthermore, the trivalent cobalt complexes were kinetically inert, but had enough strength to stabilize the intermolecular crosslinked networks. This strategy can easily be extended to other metal ions. Peng *et al.* reported a redox-responsive gel–sol transition system with an aqueous poly(acrylic acid) (PAA) solution containing trivalent cations, such as Fe(III) and Al(III).<sup>48</sup> The PAA chains in aqueous solution were joined together to form a hydrogel through binding with trivalent ferric ions. When the gel was irradiated under sunlight, the Fe(III) ion was reduced to the Fe(II) ion in the presence of citric acid. The latter cannot crosslink PAA chains any more, thus resulting in the gel to sol transition. Inversely, sol to gel transition was observed if the Fe(II)/PAA polymer solution was exposed to oxygen. Pfister and Fraser found the opposite phenomenon. Bipyridyl-centered poly(ethylene glycol) (PEG) formed hydrogels in aqueous FeSO<sub>4</sub> solutions because of the formation of coordination complexes.<sup>77</sup> However, exposure to air resulted in dissociation of these coordination hydrogels as a consequence of the oxidation of Fe(II) to Fe(III).

As well as the polymer ligands, small ligands with metal-binding sites also have the ability to form hydrogels. A coordination-based nanocomposite hydrogel was synthesized by the addition of 4,6-bis(2-pyridyl)-1,3,5-triazin-2-ol to an aqueous solution of Cu<sub>2</sub>(OAc)<sub>4</sub> in various molar ratios. The hydrogel obtained was responsive to different stimuli, such as temperature, pH and concentration.<sup>78</sup> The pincer terpyridine ligand **L15** can react with CuCl<sub>2</sub>·2H<sub>2</sub>O (molar ratio is 1 : 1) in water, leading to the formation of stable hydrogels (Fig. 12).<sup>79</sup> However, no gel formation was found when the same ligand was mixed with other Cu(II) salts, such as CuBr<sub>2</sub>, CuSO<sub>4</sub>, Cu(NO<sub>3</sub>)<sub>2</sub>, Cu(OAc)<sub>2</sub>, and Cu(OTf)<sub>2</sub>, indicating that the gel formation is highly anion-selective. The crystal structure observed from the metallo-gels revealed that the 1 : 1 metal complex with a flat conformation formed a primary dimer *via* a strong  $\pi$ – $\pi$

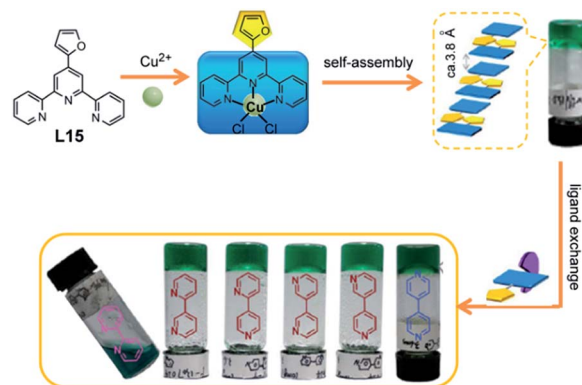


Fig. 12 Molecular structure of **L15**, and the schematic representation of the polymeric hydrogels. Reproduced with permission from ref. 79 and 80. Copyright 2013 American Chemical Society and 2014 Royal Society of Chemistry.

interaction between the furan and the central pyridine rings, which further assembled into 1-D fibers with the help of metal–metal interaction and additional  $\pi$ – $\pi$  stacking between the two side pyridine rings (Fig. 12). It is possible that the 1-D structures are significantly hampered by large sized counter anions. With this metallo-hydrogel prepared, the researchers went on to explore its dynamic features by replacing the chloride ligands with additional ones, such as 2,2′-, 2,3′-, 2,4′-, 3,3′-, 3,4′-, and 4,4′-bipyridines.<sup>80</sup> It was interesting that the metallo-hydrogel showed selective discrimination of 2,2′-bipyridine through gel–sol transition, as shown in Fig. 12. Furthermore, when 2,2′-azopyridine was used to substitute the chloride ligands of the metallo-hydrogel, a photo-switchable two-component metallo-hydrogel system could be obtained.

A polymeric hydrogel with enhanced fluorescence has been fabricated through a coordination interaction between *N*-(7-hydroxyl-4-methyl-8-coumarinyl)-glycine (**L16**) and the Zn<sup>2+</sup> ion.<sup>81</sup> When a basic aqueous solution of **L16** was reacted with Zn(OAc)<sub>2</sub>, a stable hydrogel with a strong blue emission at 440 nm was formed instantly (Fig. 13). The as-prepared hydrogel was pH sensitive and converted to a colourless solution at pH = 2 because the protonation of the ligand resulted in the blocking of the coordination site, and thus, the disruption of the hydrogel. Therefore, a drastic decrease in fluorescence was

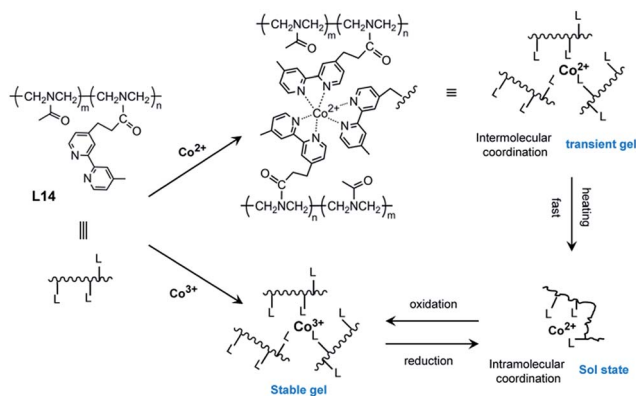


Fig. 11 Schematic representation of the redox-active coordination polymers consisting of **L14** and cobalt ions. Reproduced with permission from ref. 76. Copyright 1993 American Chemical Society.

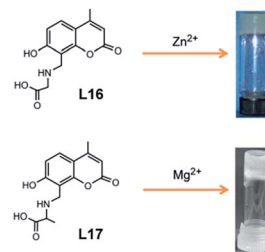


Fig. 13 Molecular structures of **L16** and **L17**, and the photo images of the resultant coordination hydrogels. Reproduced with permission from ref. 81 and 82. Copyright 2008 Royal Society of Chemistry and 2008 Wiley-VCH.

observed. Later, the authors extended their investigation to a coordination polymer system containing  $Mg^{2+}$  with a rational molecular design.<sup>82</sup> An opaque hydrogel with a strong blue emission was obtained when a basic aqueous solution of **L17** was reacted with an aqueous solution of  $Mg(CH_3COO)_2 \cdot 4H_2O$  with a metal to ligand ratio of 1 : 1. Controlled experiments showed that the rigidification of the media upon gelation slowed down the non-radiative decay processes, leading to luminescence enhancement. The hydrogel converted to a yellowish clear solution at pH 2, but retained its gel structure at pH 8 indicating pH responsive properties. Lee *et al.* also investigated the fluorescent properties of the tetrazole-based coordination polymer gel with  $Mg^{2+}$  ions.<sup>83</sup> The authors proposed that the formation of a hydrogel in its aggregate state increased the rigidity of a molecule and restricted the rotational and vibrational movements of the molecules. The limited molecular motions suppressed the internal conversion of excited molecules and slowed down non-radiative decay process, thus leading to the luminescence enhancement. In another example, the authors designed a responsive coordination hydrogel as a drug-release system triggered by pH.<sup>84</sup> Curcumin (or diferuloylmethane) molecules were encapsulated in a  $Cu^{2+}$ -contained coordination hydrogel. When the pH was adjusted to 5, almost all the curcumin molecules were released into the aqueous phase over 80 min, indicating that the curcumin encapsulated in a coordination hydrogel could be effectively released by pH control.

## 5 Application of the coordination polymer in aqueous solution

Coordination polymers with dynamic self-assemblies and physical properties in water are ideal candidates for developing fluorescence sensors and/or bio-imaging agents. A coordination polymer was firstly synthesized by Kimizuka *et al.* by mixing aqueous  $GdCl_3$  or  $TbCl_3$  with equimolar adenosine monophosphate (**L18**) in (2-[4-(hydroxyethyl)-1-piperazinyl]ethanesulfonic acid) buffer (pH = 7.4) solution.<sup>85</sup> The polymer obtained could be dispersed in water with the help of poly(sodium-4-styrene sulfonate), and formed nanoparticles with a diameter of  $41 \pm 5$  nm. As shown in Fig. 14a, the polymeric nanoparticles were formed by the coordination interaction among the nucleobases, phosphate groups and lanthanide ions. Comparing the polymer nanoparticles with a commercially available contrast agent  $[Gd(DTPA)(H_2O)]^{2-}$ , the  $Gd^{3+}/L18$  polymer nanoparticles exhibited enhanced magnetic resonance imaging properties because the  $Gd^{3+}$  ions in the nanoparticles were expected to increase the rotational correlation time  $\tau_R$ , which would improve the relaxivity per  $Gd^{3+}$  ion. Very interestingly, the supramolecular networks of nucleotide/lanthanide showed adaptive inclusion of anionic guests, including anionic dyes, gold nanoparticles, anionic proteins and cells, by coordination interactions between the lanthanide ions and the guest materials. The authors demonstrated that the coordination network with an adaptive inclusion ability could also act as scaffolds for cellular uptake and enzyme immobilization.

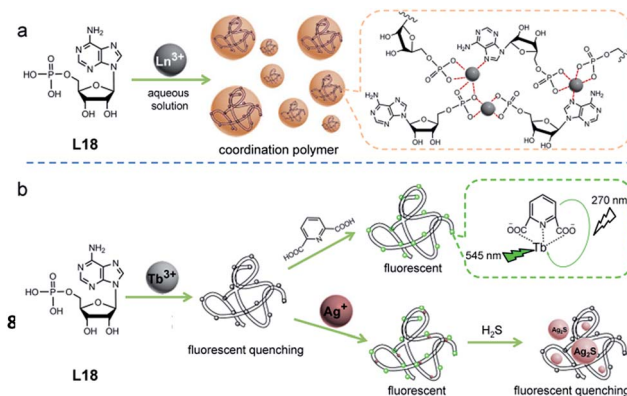


Fig. 14 (a) Molecular structure of **L18** and the resultant coordination polymers ( $Ln^{3+}/L18$ ); (b) schematic illustrations of the coordination polymer  $Tb^{3+}/L18$  acting as luminescent sensors. Reproduced with permission from ref. 85, 86 and 88. Copyright 2009, 2013 American Chemical Society, and 2014 Elsevier.

Chen *et al.* utilized the  $Tb^{3+}/L18$  coordination polymer as a receptor platform to directly detect the anthrax biomarker (dipicolinic acid, DPA) in aqueous solution.<sup>86</sup> The polymer nanoparticles were dispersed in water to form a suspension with a very weak fluorescence emission because of the quench effect caused by the O–H vibration of the coordination water molecules. In the presence of DPA, however, the fluorescence intensity of the polymer could be increased significantly because of the coordination of DPA with  $Tb^{3+}$  (Fig. 14b). The authors highlighted that the coordination of DPA with  $Tb^{3+}$  not only led to the removal of coordinated water molecules, but also offered an effective energy-transfer process from DPA to  $Tb^{3+}$ , causing enhanced fluorescence. Beside the DPA detection, the fluorescence of the  $Tb^{3+}/L18$  polymer was also responsive to  $Ag^+$  ions.<sup>87</sup> Upon addition of  $Ag^+$ , the fluorescence intensity of the polymer suspension was increased significantly because of the coordination of  $Ag^+$  to **L18** causing an alteration of the excited state of **L18** and a more effective energy transfer from **L18** to  $Tb^{3+}$  (Fig. 14b). The emission intensity of the fluorescent polymer is pH dependent. At pH 7.4, the intensity reached the maximum. A very acidic or basic medium weakened the fluorescence intensity because of the dissociation of the coordination polymer caused by the protonation of the ligands or the formation of terbium hydrate. In addition, the coordination polymer showed high selectivity for  $Ag^+$  compared to other metal ions, such as  $Ca^{2+}$ ,  $Cd^{2+}$ ,  $Co^{2+}$ ,  $Cr^{2+}$ ,  $Cu^{2+}$ ,  $Fe^{2+}$ ,  $Fe^{3+}$ ,  $Hg^+$ ,  $Hg^{2+}$ ,  $K^+$ ,  $Mg^{2+}$ ,  $Mn^{2+}$ ,  $Na^+$ ,  $Ni^{2+}$  and  $Pb^{2+}$ . This might be ascribed to the fact that the d electrons of  $Ag^+$  in the valence orbital cause a metal-to-ligand charge transfer, which sensitized the fluorescence of  $Tb^{3+}$ . However, in the presence of sulfide, the emission intensity of the fluorescent polymer was reduced strongly within 2 min because the formation of  $Ag_2S$  caused the dissociation of the coordination bond between the  $Ag^+$  and **L18** (Fig. 14b).<sup>88</sup> Systematic investigations showed that only sulfide can produce a significant fluorescence quenching. Therefore, the coordination polymer could be utilized as a fluorescent sensor to detect sulfide in human serum. The lowest detectable concentration of

sulfide in serum is approximately 0.8  $\mu\text{M}$  (signal/noise ratio > 3 : 1). This demonstrated that the fluorescent coordination polymer has particular advantages for detecting sulfide in biological systems, such as tissue fluids, blood, and urine. Subsequently, the researchers developed a series of  $\text{Tb}^{3+}$ -contained coordination polymers for detecting  $\text{Hg}^{2+}$  and ciprofloxacin in aqueous solution.<sup>89,90</sup>

Recently, Liu and Liu have created a fluorescence sensor from a sophisticated molecular design.<sup>91</sup> The researchers start from a polymerizable quinolone-based monomer with the 2-position substituted with a methyl group and the 8-position modified with a toluenesulfonamido moiety. Then a hydrophilic block copolymer was connected to the quinolone-based monomer to improve the water-solubility. The non-fluorescent ligand (**L19**) obtained was dissolved in water and selectively bound with  $\text{Zn}^{2+}$  ions, leading to the formation of a coordination polymer with enhanced fluorescence at 482 nm (Fig. 15). The polymer self-assembled into micelles possessing quinolone-based cores and PEG coronas upon heating to above the LCST (37 °C), and the fluorescence intensity exhibited a 6-fold increase because of the fact that quinolone moieties were located in a more hydrophobic microenvironment. The fluorescence emission of the coordination polymer aqueous solution at 37 °C is dramatically quenched upon the addition of EDTA. A reversible on/off switchable fluorescence emission was observed at 37 °C upon sequential addition of  $\text{Zn}^{2+}$  and EDTA. The authors pointed out that the high temperature decreased the binding affinity between  $\text{Zn}^{2+}$  and the quinolone groups, which was favourable for the complete binding between  $\text{Zn}^{2+}$  and EDTA. The detection selectivity of the polymer toward  $\text{Zn}^{2+}$  ions over other common metal ions was then investigated. It was found that among a series of metal ions including  $\text{Ag}^+$ ,  $\text{Al}^{3+}$ ,  $\text{Ba}^{2+}$ ,  $\text{Ca}^{2+}$ ,  $\text{Cd}^{2+}$ ,  $\text{Co}^{2+}$ ,  $\text{Cu}^{2+}$ ,  $\text{Fe}^{2+}$ ,  $\text{Fe}^{3+}$ ,  $\text{Hg}^{2+}$ ,  $\text{Li}^+$ ,  $\text{Mg}^{2+}$ ,  $\text{Mn}^{2+}$ ,  $\text{Ni}^{2+}$ ,  $\text{Pb}^{2+}$  and  $\text{Zn}^{2+}$ , only  $\text{Zn}^{2+}$

ions exhibited the most prominent enhancement (15-fold). The presence of 4.0 equiv.  $\text{Cd}^{2+}$  induces 8.7-fold emission. Important bio-related metal ions such as  $\text{Ca}^{2+}$ ,  $\text{K}^+$ ,  $\text{Mg}^{2+}$  and  $\text{Na}^+$ , in most living cells resulted in negligible fluorescence enhancement, indicating that the fluorescent polymer has potential for bio-imaging analysis. *In vitro* fluorescence imaging studies further suggested that the micelles can effectively enter into living HeLa cells and efficiently recognize and capture  $\text{Zn}^{2+}$  ions to give prominently enhanced fluorescence emissions (Fig. 15).

In fact, the coordination centers of many coordination polymers usually possess charges,<sup>92</sup> which provide additional opportunities for the fabrication of hierarchical nanostructures through co-assembly with other complementary components *via* Coulomb interaction.<sup>93</sup> Yan *et al.* synthesized a coordination polymer firstly by mixing ligand L2-4 with  $\text{Fe}^{2+}$ . Upon addition of the positively charged copolymer P2VP<sub>41</sub>-*b*-PEO<sub>205</sub> to the above aqueous solution of coordination polymers, micellar structures were obtained because of the electrostatic attraction between the negatively charged coordination centers and the positively charged pyridinium segments (Fig. 16).<sup>94</sup> Significantly, the micellar polymer underwent a reversible redox process, which caused a change of the magnetic properties of the systems. For example, diamagnetic micelles in the reduction state ( $\text{Fe}^{2+}$ ) could transform into paramagnetic micelles ( $\text{Fe}^{3+}$ ) upon addition of  $\text{H}_2\text{O}_2$ , resulting in a smart magnetic resonance imaging contrast agent. In a further step, the authors firstly prepared the coordination polymer starting from  $\text{Fe}^{3+}$ , L2-4 and P2VP<sub>41</sub>-*b*-PEO<sub>205</sub>.<sup>95</sup> In the presence of  $\text{NaBH}_4$ , the neutral micelles have the propensity to change into their reduced state,  $\text{Fe}^{2+}$ , simultaneously producing negatively charged cores (Fig. 16). The fraction of negative charges ( $f^-$ ) in the reduced micelles can be described as follows:  $f^- = [-]/([-] + [+])$ , where  $[-]$  is the molar concentration of the negative elementary charges carried by the reduced coordination polymers, and  $[+]$  is that of the positive charges carried by the P2VP<sub>41</sub> block of the diblock copolymers. The reduced micelles carrying negative charges have the ability to further uptake oppositely charged

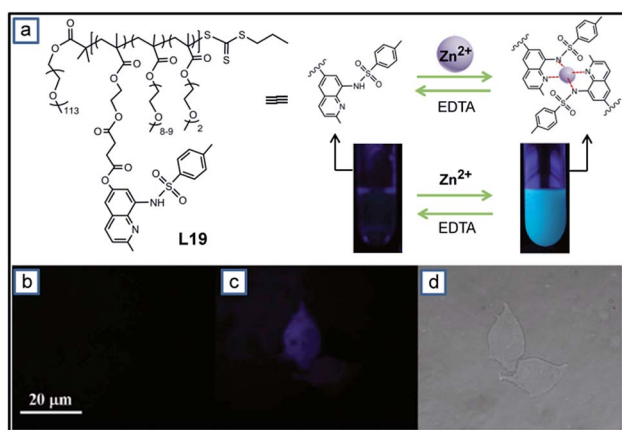


Fig. 15 (a) Molecular structure of **L19** and the schematic illustrations of the luminescent coordination polymer; (b) fluorescent image of HeLa cells incubated with 2.0 g L<sup>-1</sup> **L19** at 37 °C for 4 h, (c) fluorescent image of HeLa cells incubated with 2.0 g L<sup>-1</sup> **L19** at 37 °C for 4 h and followed by addition of 200  $\mu\text{M}$   $\text{Zn}^{2+}$  ions, and (d) a bright field image of the cells in panel (c). Reproduced with permission from ref. 91. Copyright 2011 American Chemical Society.

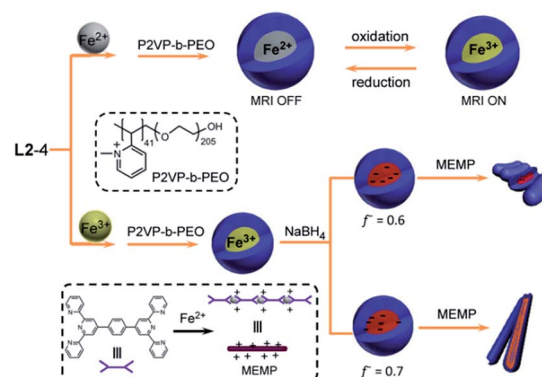


Fig. 16 Schematic illustrations of the hierarchical nanostructures through co-assembly of coordination polymers ( $\text{Fe}^{2+}/\text{L2-4}$  or  $\text{Fe}^{3+}/\text{L2-4}$ ) with oppositely charged polymers, and their dynamic features. Reproduced with permission from ref. 94 and 95. Copyright 2012 American Chemical Society and 2010. Royal Society of Chemistry.

species. The researchers performed the reduction-triggered uptake of positively charged coordination polymers (MEPE) into micelles. As shown in Fig. 16, after addition of MEPE to reduced micelles with  $f^- = 0.6$ , the global micelles changed into banana-bundle-like ones due to the rigidity of MEPE. However, when the reduced micelles with  $f^- = 0.7$  were used as a starting configuration, one could observe the formation of fiber-like structures upon sequestering the MEPE. It is clear that the lower quantity of  $f^-$  in the reduced micelles can only take up a small amount of rigid MEPE. This means that the deformation of the global micelles is not as significant as that in higher  $f^-$  systems. Lately, the authors successfully selected a negatively charged fluorescent dye, eosin B, as a model cargo to track the release and uptake process.<sup>96</sup> The results demonstrated that the co-assembled polymer micelles have an important potential as a redox-gated micellar carrier for uptake and release of charged cargos.

## 6 Conclusions

The fusion of coordination chemistry and polymer science has shown astonishing growth. In this review, we describe the dynamic self-assembly of coordination polymers in aqueous solution with the aim of developing smart materials. Selected monomer or polymer ligands carrying pyridine, tetrazole, carboxylic and amino acid moieties have been employed to bind various metal ions. The resultant coordination polymers are kinetically labile in water, which endows this system with stimuli-responsiveness. Systematic studies reveal that the self-assembly behavior of the coordination polymers provides powerful tools to create dynamic nanostructures in aqueous solution, including expansion-contraction of helix and micelles, switchable tubules and 2-D flat sheets. Although the knowledge of how the small environmental variations, including pH, redox reactions, ligand exchange, anion exchange, temperature and photosensitivity, can be judiciously chosen to affect the dynamic self-assemblies of coordination polymers is accumulated, ongoing research work is still necessary for the rational design of coordination polymers. In particular, functional groups can be incorporated into the organic ligands to offer new opportunities in developing multi-responsive nanostructures in water for mimicking the structures and functions of natural biopolymers.

Beyond the traditional focus on the structural features, a more important issue is the dynamic physical properties of the coordination polymers arising from the requirements for potential applications deriving from the presence of metal ions. The dynamic features of the coordination polymers are beginning to show significant potential in for their use as sensors and bio-imaging agents. In fact, many metal ions are luminescent, magnetic, redox active, photosensitive or have catalytic properties, consequently, the possibility of modifying their physical properties as well as their nanostructures by choosing the metal ions and the ligands to be used may help them find many practical applications beyond sensors or bio-imaging agents.

## Acknowledgements

We gratefully acknowledge the National Science Foundation of China (50973042), Sci-Tech Development Project of Jilin Province (20130522133JH). Prof. M. Lee thanks 111 project of China (B06009), NSFC (21221063) and the "Recruitment Program of Foreign Experts" (2014).

## Notes and references

- 1 C. Fouquey, J.-M. Lehn and A.-M. Levelut, *Adv. Mater.*, 1990, **5**, 254–257.
- 2 F. Huang and H. W. Gibson, *J. Am. Chem. Soc.*, 2004, **126**, 14738–14739.
- 3 T. Aida, E. W. Meijer and S. I. Stupp, *Science*, 2012, **335**, 813–817.
- 4 Y. Liu, Y. Yu, J. Gao, Z. Wang and X. Zhang, *Angew. Chem., Int. Ed.*, 2010, **49**, 6576–6579.
- 5 M. J. Mayoral, C. Rest, V. Stepanenko, J. Schellheimer, R. Q. Albuquerque and G. Fernández, *J. Am. Chem. Soc.*, 2013, **135**, 2148–2151.
- 6 X. Ji, K. Zhu, X. Yan, Y. Ma, J. Li, B. Hu, Y. Yu and F. Huang, *Macromol. Rapid Commun.*, 2012, **33**, 1197–1202.
- 7 A. Harada, Y. Takashima and H. Yamaguchi, *Chem. Soc. Rev.*, 2009, **38**, 875–882.
- 8 J.-M. Lehn, *Polym. Int.*, 2002, **51**, 825–839.
- 9 X. Yan, F. Wang, B. Zheng and F. Huang, *Chem. Soc. Rev.*, 2012, **41**, 6042–6065.
- 10 J. Cortese, C. Soulié-Ziakovic, S. Tencé-Girault and L. Leibler, *J. Am. Chem. Soc.*, 2012, **134**, 3671–3674.
- 11 T. H. Rehm and C. Schmuck, *Chem. Soc. Rev.*, 2010, **39**, 3597–3611.
- 12 L. Liang, Y. Zhao, K. Chen, X. Xiao, J. K. Clegg, Y.-Q. Zhang, Z. Tao, S.-F. Xue, Q.-J. Zhu and G. Wei, *Polymer*, 2013, **5**, 418–430.
- 13 Z.-Y. Li, Y. Zhang, C.-W. Zhang, L.-J. Chen, C. Wang, H. Tan, Y. Yu, X. Li and H.-B. Yang, *J. Am. Chem. Soc.*, 2014, DOI: 10.1021/ja413047r, ASAP.
- 14 F. S. Han, M. Higuchi and D. G. Kurth, *Adv. Mater.*, 2007, **19**, 3928–3931.
- 15 R. Nishiyabu, C. Aimé, R. Gondo, T. Noguchi and N. Kimizuka, *Angew. Chem., Int. Ed.*, 2009, **48**, 9465–9468.
- 16 J. Benjamin Beck and S. J. Rowan, *J. Am. Chem. Soc.*, 2003, **125**, 13922–13923.
- 17 J. Brassinne, C.-A. Fustin and J.-F. Gohy, *J. Inorg. Organomet. Polym.*, 2013, **23**, 24–40.
- 18 J. Paulusse, J. Huijbers and R. Sijbesma, *Macromolecules*, 2005, **38**, 6290–6298.
- 19 U. Velten and M. Rehahn, *Chem. Commun.*, 1996, 2639–2640.
- 20 L. Brunsveld, B. J. B. Folmer, E. W. Meijer and R. P. Sijbesma, *Chem. Rev.*, 2001, **101**, 4071–4098.
- 21 J. Paulusse, J. Huijbers and R. Sijbesma, *Chem.–Eur. J.*, 2006, **12**, 4928–4934.
- 22 N. Giri and S. L. James, *Chem. Commun.*, 2011, **47**, 1458–1460.
- 23 A. K. Miller, Z. Li, K. A. Streltzyk, A. M. Jamieson and S. J. Rowan, *Polym. Chem.*, 2012, **3**, 3132–3138.

- 24 S. Schmatloch, A. van den Berg, M. Fijten and U. Schubert, *Macromol. Rapid Commun.*, 2004, **25**, 321–325.
- 25 K. P. Nair, V. Breedveld and M. Weck, *Macromolecules*, 2011, **44**, 3346–3357.
- 26 T. Fukino, H. Joo, Y. Hisada, M. Obana, H. Yamagishi, T. Hikima, M. Takata, N. Fujita and T. Aida, *Science*, 2014, **344**, 499–504.
- 27 W. Weng, J. Benjamin Beck, A. M. Jamieson and S. J. Rowan, *J. Am. Chem. Soc.*, 2006, **128**, 11663–11672.
- 28 P. Wei, B. Xia, Y. Zhang, Y. Yu and X. Yan, *Chem. Commun.*, 2014, **50**, 3973–3975.
- 29 U. S. Schubert and C. Eschbaumer, *Angew. Chem., Int. Ed.*, 2002, **41**, 2892–2926.
- 30 C. R. South, C. Burd and M. Weck, *Acc. Chem. Res.*, 2007, **40**, 63–74.
- 31 Y. Yan and J. B. Huang, *Coord. Chem. Rev.*, 2010, **354**, 1072–1080.
- 32 V. A. Friese and D. G. Kurth, *Curr. Opin. Colloid Interface Sci.*, 2009, **14**, 81–93.
- 33 J. H. Jung, J. H. Lee, J. R. Silverman and G. John, *Chem. Soc. Rev.*, 2013, **42**, 924–936.
- 34 A. O. Moughton and R. K. O'Reilly, *Macromol. Rapid Commun.*, 2010, **31**, 37–52.
- 35 G. R. Whittell and I. Manners, *Adv. Mater.*, 2007, **19**, 3439–3468.
- 36 X. Wang and R. McHale, *Macromol. Rapid Commun.*, 2010, **31**, 331–350.
- 37 J. Howard and A. A. Hyman, *Nature*, 2003, **422**, 753–758.
- 38 H. Y. Kueh and T. J. Mitchison, *Science*, 2009, **325**, 960–963.
- 39 D. Ghosh and V. L. Pecoraro, *Curr. Opin. Chem. Biol.*, 2005, **9**, 97–103.
- 40 S. N. Dublin and V. P. Conticello, *J. Am. Chem. Soc.*, 2008, **130**, 49–51.
- 41 C. M. Micklitsch, P. J. Knerr, M. C. Branco, R. Nagarkar, D. J. Pochan and J. P. Schneider, *Angew. Chem., Int. Ed.*, 2011, **50**, 1577–1579.
- 42 P. Anzini, C. Xu, S. Hughes, E. Magnotti, T. Jiang, L. Hemmingsen, B. Demeler and V. P. Conticello, *J. Am. Chem. Soc.*, 2013, **135**, 10278–10281.
- 43 X. I. Ambroggio and B. Kuhlman, *J. Am. Chem. Soc.*, 2006, **128**, 1154–1161.
- 44 J. Dong, J. E. Shokes, R. A. Scott and D. G. Lynn, *J. Am. Chem. Soc.*, 2006, **128**, 3540–3542.
- 45 T. Vermonden, J. van der Gucht, P. de Waard, A. T. M. Marcelis, N. A. M. Besseling, E. J. R. Sudhölter, G. J. Fleer and M. A. Cohen Stuart, *Macromolecules*, 2003, **36**, 7035–7044.
- 46 S. J. Buwalda, P. J. Dijkstra and J. Feijen, *J. Polym. Sci., Part A: Polym. Chem.*, 2012, **50**, 1783–1791.
- 47 M. Chiper, A. Winter, R. Hoogenboom, D. A. M. Egbe, D. Wouters, S. Hoepfener, C.-A. Fustin, J.-F. Gohy and U. S. Schubert, *Macromolecules*, 2008, **41**, 8823–8831.
- 48 F. Peng, G. Li, X. Liu, S. Wu and Z. Tong, *J. Am. Chem. Soc.*, 2008, **130**, 16166–16167.
- 49 D. E. Fullenkamp, L. He, D. G. Barrett, W. R. Burghardt and P. B. Messersmith, *Macromolecules*, 2013, **46**, 1167–1174.
- 50 D.-H. Li, J.-S. Shen, N. Chen, Y.-B. Ruan and Y.-B. Jiang, *Chem. Commun.*, 2011, **47**, 5900–5902.
- 51 J. van der Gucht, N. A. M. Besseling and H. P. van Leeuwen, *J. Phys. Chem. B*, 2004, **108**, 2531–2539.
- 52 T. Vermonden, W. M. de Vos, A. T. M. Marcelis and E. J. R. Sudhölter, *Eur. J. Inorg. Chem.*, 2004, 2847–2852.
- 53 T. Vermonden, M. J. van Steenbergen, N. A. M. Besseling, A. T. M. Marcelis, W. E. Hennink, E. J. R. Sudhölter and M. A. Cohen Stuart, *J. Am. Chem. Soc.*, 2004, **126**, 15802–15808.
- 54 J.-F. Gohy, B. G. G. Lohmeijer and U. S. Schubert, *Macromolecules*, 2002, **35**, 4560–4563.
- 55 J.-F. Gohy, B. G. G. Lohmeijer and U. S. Schubert, *Macromol. Rapid Commun.*, 2002, **23**, 555–560.
- 56 J.-F. Gohy, B. G. G. Lohmeijer, S. K. Varshney, B. Décamps, E. Leroy, S. Boileau and U. S. Schubert, *Macromolecules*, 2002, **35**, 9748–9755.
- 57 M. Chiper, D. Fournier, R. Hoogenboom and U. S. Schubert, *Macromol. Rapid Commun.*, 2008, **29**, 1640–1647.
- 58 G. Gröger, W. Meyer-Zaika, C. Böttcher, F. Gröhn, C. Ruthard and C. Schmuck, *J. Am. Chem. Soc.*, 2011, **133**, 8961–8971.
- 59 S. Biswas, K. Kinbara, N. Oya, N. Ishii, H. Taguchi and T. Aida, *J. Am. Chem. Soc.*, 2009, **131**, 7556–7557.
- 60 T. Sendai, S. Biswas and T. Aida, *J. Am. Chem. Soc.*, 2013, **135**, 11509–11512.
- 61 J.-M. Lehn, *Rep. Prog. Phys.*, 2004, **67**, 249–265.
- 62 E. Yashima, K. Maeda and Y. Furusho, *Acc. Chem. Res.*, 2008, **41**, 1166–1180.
- 63 J. Fei, L. Gao, J. Zhao, C. Du and J. B. Li, *Small*, 2013, **9**, 1021–1024.
- 64 H. Maeda, T. Nishimura, R. Akuta, K. Takaishi, M. Uchiyama and A. Muranaka, *Chem. Sci.*, 2013, **3**, 1204–1211.
- 65 O.-S. Jung, Y. J. Kim, Y.-A. Lee, J. K. Park and H. K. Chae, *J. Am. Chem. Soc.*, 2000, **122**, 9921–9925.
- 66 M. Numata, D. Kinoshita, N. Hirose, T. Kozawa, H. Tamiaki, Y. Kikkawa and M. Kanetsato, *Chem.–Eur. J.*, 2013, **19**, 1592–1598.
- 67 H.-J. Kim, E. Lee, H.-S. Park and M. Lee, *J. Am. Chem. Soc.*, 2007, **129**, 10994–10995.
- 68 J.-S. Shen, D.-H. Li, M.-B. Zhang, J. Zhou, H. Zhang and Y.-B. Jiang, *Langmuir*, 2011, **27**, 481–486.
- 69 H.-J. Kim, J.-H. Lee and M. Lee, *Angew. Chem., Int. Ed.*, 2005, **44**, 5810–5814.
- 70 S. Shin, S. Lim, Y. Kim, T. Kim, T.-L. Choi and M. Lee, *J. Am. Chem. Soc.*, 2013, **135**, 2156–2159.
- 71 W. Li, I.-S. Park, S.-K. Kang and M. Lee, *Chem. Commun.*, 2012, **48**, 8796–8798.
- 72 C. Tsitsilianis, *Soft Matter*, 2010, **6**, 2372–2388.
- 73 Y. Qiao, Y. Lin, S. Zhang and J. Huang, *Chem.–Eur. J.*, 2011, **17**, 5180–5187.
- 74 Y. Pan, Y. Gao, J. Shi, L. Wang and B. Xu, *J. Mater. Chem.*, 2011, **21**, 6804–6806.
- 75 R. Gavara, J. Llorca, J. C. Lima and L. Rodríguez, *Chem. Commun.*, 2013, **49**, 72–74.
- 76 Y. Chujo, K. Sada and T. Saegusa, *Macromolecules*, 1993, **26**, 6320–6323.

- 77 A. Pfister and C. L. Fraser, *Biomacromolecules*, 2006, **7**, 459–468.
- 78 J.-J. Wu, M.-L. Cao, J.-Y. Zhang and B.-H. Ye, *RSC Adv.*, 2012, **2**, 12718–12723.
- 79 W. Fang, Z. Sun and T. Tu, *J. Phys. Chem. C*, 2013, **117**, 25185–25194.
- 80 W. Fang, X. Liu, Z. Lu and T. Tu, *Chem. Commun.*, 2014, **50**, 3313–3316.
- 81 W. L. Leong, A. Y.-Y. Tam, S. K. Batabyal, L. W. Koh, S. Kasapis, V. W.-W. Yam and J. J. Vittal, *Chem. Commun.*, 2008, 3628–3630.
- 82 W. L. Leong, S. K. Batabyal, S. Kasapis and J. J. Vittal, *Chem. – Eur. J.*, 2008, **14**, 8822–8829.
- 83 J. H. Lee, H. Lee, S. Seo, J. Jaworski, M. L. Seo, S. Kang, J. Y. Lee and J. H. Jung, *New J. Chem.*, 2011, **35**, 1054–1059.
- 84 H. Lee, J. H. Lee, S. Kang, J. Y. Lee, G. John and J. H. Jung, *Chem. Commun.*, 2011, **47**, 2937–2939.
- 85 R. Nishiyabu, N. Hashimoto, T. Cho, K. Watanabe, T. Yasunaga, A. Endo, K. Kaneko, T. Niidome, M. Murata, C. Adachi, Y. Katayama, M. Hashizume and N. Kimizuka, *J. Am. Chem. Soc.*, 2009, **131**, 2151–2158.
- 86 H. Tan, C. Ma, L. Chen, F. Xu, S. Chen and L. Wang, *Sens. Actuators, B*, 2014, **190**, 621–626.
- 87 H. Tan and Y. Chen, *Chem. Commun.*, 2011, **47**, 12373–12375.
- 88 B. Liu and Y. Chen, *Anal. Chem.*, 2013, **85**, 11020–11025.
- 89 H. Tan, B. Liu and Y. Chen, *ACS Nano*, 2012, **6**, 10505–10511.
- 90 H. Tan, L. Zhang, C. Ma, Y. Song, F. Xu, S. Chen and L. Wang, *ACS Appl. Mater. Interfaces*, 2013, **5**, 11791–11796.
- 91 T. Liu and S. Liu, *Anal. Chem.*, 2011, **83**, 2775–2785.
- 92 V. A. Friese and D. G. Kurth, *Coord. Chem. Rev.*, 2008, **252**, 199–211.
- 93 L. Xu, L. Jiang, M. Drechsler, Y. Sun, Z. Liu, J. B. Huang, B. Z. Tang, Z. Li, M. A. Cohen Stuart and Y. Yan, *J. Am. Chem. Soc.*, 2014, **136**, 1942–1947.
- 94 Y. Yan, Y. Lan, A. de Keizer, M. Drechsler, H. Van As, M. A. Cohen Stuart and N. A. M. Besseling, *Soft Matter*, 2010, **6**, 3244–3248.
- 95 Y. Ding, Y. Yang, L. Yang, Y. Yan, J. B. Huang and M. A. Cohen Stuart, *ACS Nano*, 2012, **6**, 1004–1010.
- 96 L. Zhao, Y. Yan and J. B. Huang, *Langmuir*, 2012, **28**, 5548–5554.